Journal of Energetic Materials
Publication details, including instructions for authors and subscription information:
http://www.informaworld.com/smpp/title~content=t713770432

Reactive flow modeling of recent embedded gauge and metal acceleration experiments on detonating PBX-9404 and LX-17

C. M. Tarver[a]; N. L. Parker[a]; H. G. Palmer[a]; B. Hayes[a]; L. M. Erickson[a]
[a] Lawrence Livermore National Laboratory University of California, Livermore, California

To cite this Article Tarver, C. M. , Parker, N. L. , Palmer, H. G. , Hayes, B. and Erickson, L. M.(1983) 'Reactive flow modeling of recent embedded gauge and metal acceleration experiments on detonating PBX-9404 and LX-17', Journal of Energetic Materials, 1: 3, 213 — 250
To link to this Article: DOI: 10.1080/07370658308010620
URL: http://dx.doi.org/10.1080/07370658308010620

REACTIVE FLOW MODELING OF RECENT EMBEDDED GAUGE AND METAL ACCELERATION EXPERIMENTS ON DETONATING PBX-9404 and LX-17

C. M. Tarver, N. L. Parker, H. G. Palmer
B. Hayes and L. M. Erickson

Lawrence Livermore National Laboratory
University of California
Livermore, California 94550

ABSTRACT

The ignition and growth model of the reactive flow during shock initiation and detonation wave propagation in the heterogeneous solid explosives PBX-9404 and LX-17 is compared to recent embedded particle velocity and stress gauge measurements in detonating PBX-9404 and Fabry-Perot free surface velocity measurements of thin metal plates accelerated by detonating PBX-9404 and LX-17. The overall agreement between the numerical calculations and the various experimental records, which have time resolutions in the nanosecond regime, is very good. The regions of disagreement emphasize some of the processes involved in reactive flow and metal acceleration that are not fully understood and directions for future experimental and modeling work. These new experimental and calculational results are also compared to some previously reported back surface particle velocity gauge and free surface

Journal of Energetic Materials Vol. 1, 213-250

Published in 1983 by Dowden, Brodman & Devine, Inc.

velocity measurements for detonating PBX-9404. The experimental records and the numerical results clearly demonstrate that detonating PBX-9404 attains particle velocities and pressures in excess of the Chapman-Jouguet (CJ) values in less than ten millimeters after detonation has been established and that the resulting detonation reaction zone has a steady profile for its entire length of propagation.

INTRODUCTION

The ignition and growth model[1] of reactive flow during shock initiation and detonation wave propagation has successfully calculated a great deal of one- and two-dimensional experimental data on solid heterogeneous explosives and propellants,[2-6] particularly on the HMX-based explosive PBX-9404[7] and the TATB-based explosive LX-17.[7] The ignition and growth model of a detonation wave is based on the Zel'dovich[8]-von Neumann[9]-Doring[10] (ZND) model, in which the steady state reaction zone consists of a leading shock wave front, a chemical reaction zone in which the shocked unreacted explosive is converted to reaction products according to a reaction rate law, and a Chapman[11]-Jouguet[12] (CJ) state at which the chemical reaction is complete and the flow is sonic. The reaction zone is followed by a non-steady rarefaction (or Taylor) wave in which the reaction products expand and cool. The equations of state and chemical reaction rates used to

model shock initiation and detonation in PBX-9404 and LX-17 are discussed by Tarver and Hallquist[2] and are listed in Table I. The descriptions of detonation wave propagation are based on the particle velocity histories measured by Hayes and Tarver[3] for PBX-9404, LX-17 and other explosives using a 25 μm thick copper gauge system with a several nanosecond time resolution developed by Hayes.[13] These particle velocity histories were all measured at a depth of 50.8 mm in the test explosive. One experimental result reported in this paper is the record of a Hayes-type particle velocity gauge at a much smaller depth of detonating PBX-9404 in a one-dimensional experiment conducted in the LLNL 101.6 mm gas gun.[14] The multiple embedded electromagnetic particle velocity gauge developed by Erickson et. al.[15] for shock initiation studies is also used to study detonating PBX-9404 at short run distances. In this application these Erickson-type gauge packages consist of a 25 μm thick aluminum foil encapsulated in a similar thickness of teflon, thus yielding a better impedance match to the explosive than the copper Hayes-type gauge but a slightly longer time response. The two types of particle velocity gauges give excellent agreement in both inert and reacting environments. Thicker multiple particle velocity gauges have been used in detonating TNT-based[16,17] and non-ideal explosives.[16]

In addition to embedded particle velocity gauges, several groups have developed the capability of using multiple embedded manganin stress gauges to study shock initiation and detonation wave processes.[18-22] To survive for reasonable times in the turbulent flow produced in the shock to detonation transition process, the 25 μm manganin foil has to be encapsulated in a much greater thickness of teflon insulation. Thus these stress gauges perturb the reactive flow more than the particle velocity gauges, and the records are more difficult to analyze. However, a set of four embedded manganin gauge records in detonating PBX-9404 are compared to ignition and growth reactive flow model predictions in the next section of this paper.

Just as the time resolution of the embedded particle velocity gauges has recently been improved, two new techniques have been developed to study metal acceleration by detonation waves with nanosecond resolution. The Fabry-Perot technique of measuring the free surface velocity of thin metal plates driven by detonating PBX-9404 and LX-17 described by Erickson et. al.[23] is used in the paper to measure the free surface velocity histories of thin aluminum and copper plates in 101.6 mm gun experiments and the early-time radial copper wall velocities in the cylinder test.[24] The second technique is also a laser based velocity interferometer system call ORVIS

for Optically Recorded Velocity Interferometer System, in which the motion of very thin metal foils through a water medium is recorded by a high speed electronic streak camera. Sheffield et. al.[25] have measured this foil motion using ORVIS for several explosives, including the TATB-based explosive PBX-9502[7] and TNT. Al'tshuler et. al.[26] have also reported using a similar laser technique on other detonating explosives. The ignition and growth model is used in this paper to calculate the Fabry-Perot records for PBX-9404 and LX-17 and in Sheffield et. al.[25] to calculate the ORVIS records for PBX-9502 and TNT. A great deal is being learned about the equations of state and reaction rates of detonating explosives and about the equations of state and time-dependent processes in metals and other inert materials by these comparisons of experimental records and numerical modeling results. Numerical models can also be compared to previously reported metal acceleration experiments that have led to considerable controversy.[27-31] In this paper the ignition and growth model for PBX-9404 is compacted to the back surface particle velocity gauge measurements of Davis and Ramsay[32,33] and the free surface velocity measurements on thicker metal plates by Craig[34] and Cast et. al.[35] using the reflected wire technique. The main purposes of this paper are to present the new experimental data and to determine the ability of the ignition and growth model to calculate all of the available data.

EMBEDDED GAUGE RESULTS FOR PBX-9404

As discussed in the Introduction, the Hayes-type and Erickson-type embedded particle velocity gauges are now yielding good agreement in inert materials and detonating explosives. Figure 1 contains two particle velocity histories in detonating PBX-9404 using Erickson-type gauges of the thicknesses listed on Fig. 1 at depths of 10 mm and 14 mm. This experiment used a non-metallic (teflon) flyer plate impacting the PBX-9404 at 2 mm/μs and imparting approximately 8 GPa pressure at the interface. The run distance to detonation at this input pressure is 2-3 mm so the detonation wave is well established by the time it arrives at the first gauge station 10 mm into the PBX-9404. Figure 2 shows two additional Erickson-type gauge records from the same experiment at the same depths in PBX-9404 with slightly thicker teflon insulation, as listed on the Fig. 2. Also shown in Figs. 1 and 2 are the calculated particle velocity histories in the teflon just behind the aluminum gauge element. The PBX-9404 is described by the ignition and growth model using the parameters listed in Table I. The equations of state parameters for aluminum, teflon, and the other inert materials modeled in this paper are listed in Table II. The calculations reported in this paper generally use 20 zones per mm in the reacting explosive and corresponding zone dimensions for different

density and impedance inert materials. Occasionally a very finely zoned calculation with 100 zones per mm of explosive is used to resolve the reaction zone in great detail. Similar particle velocity histories are shown in Fig. 3 for a Hayes-type gauge (50 μm of copper in this experiment which had nearly identical initial conditions as the experiment described in Figs. 1 and 2) and for the calculated particle velocity history in the PBX-9404 just behind the copper gauge. This particular gauge was a thicker experimental design that did not yield as accurate a representation of the flow as the standard gauge used by Hayes and Tarver[3] (25 μm of copper). However, the agreement between the experimental records and calculated histories, which were normalized to Hayes-type gauges at a depth of 50.8 mm, in Figs. 1-3 is quite good considering the inherent time responses of these gauge packages. In particular the excellent agreement between the gauge records and calculations in the rarefaction or Taylor wave at particle velocities below 2 mm/μs proves that these gauges faithfully record the flow for more than a microsecond. Although the experimentally recorded peak particle velocities are not quite as high as the ZND model calculations in the first 0.1 μs, these records indicate that the detonation wave front in PBX-9404 attains particle velocities and pressures in excess of the CJ values in less than ten millimeters after detonation has been established.

As discussed in the Introduction, manganin stress gauges require thicker insulation than particle velocity gauges and thus perturb the reactive flow to a greater extent. However, these stress gauges do accurately record the flow associated with detonation waves in PBX-9404, as demonstrated in Fig. 4. Four manganin gauge records, each gauge consisting of 25 μm of manganin with 275 μm of teflon on each side, are shown in Fig. 4 at depths of 5, 10, 15 and 20 mm of PBX-9404 in an experiment with a stainless steel flyer plate that imparts approximately 12 GPa into the PBX-9404. The run distance to detonation is therefore 1-2 mm so even the 5 mm deep gauge should be in the detonation regime.

The calculated pressure histories in the teflon zones just behind the manganin gauge elements are also shown in Fig. 4. These calculations show the two or three peak structure created by the interaction of the gauge package materials with the detonation wave. Except for the 5 mm deep gauge record, where the presence of the relatively thick manganin gauge package seems to perturb the detonation flow more than the calculations predict, the agreement between the experimentally measured and the calculated early-time pressure peaks is excellent. The close agreement between the measured and calculated peak pressures at the 10 mm gauge is another indication that pressures in excess of the CJ values are attained in less than

ten millimeters of detonation propagation. However, the agreement in the rarefaction wave region is not as good as for the particle velocity gauges.

FABRY-PEROT MEASUREMENTS FOR DETONATING PBX-9404

The Fabry-Perot technique has been used to measure the free surface velocity of thin metal plates accelerated by detonating PBX-9404 in one-dimensional gas gun experiments and cylinder tests. In the 101.6 mm gas gun experiments, a 6 mm thick copper flyer plate impacted 17 mm of PBX-9404 at 1.25 mm/μs imparting a 9 GPa shock pressure into the PBX-9404. The resulting free surface velocity records of thin copper or aluminum plates accelerated by the detonating PBX-9404 are shown in Figs. 5, 6, and 7 for a 0.5 mm thick copper plate, a 0.5 mm thick aluminum plate, and a 0.25 mm thick copper plate, respectively. The ignition and growth calculations for each experiment are included in Fig. 5, 6, and 7. The various regions of velocity decrease or "pull-back" and subsequent reshock are resolved by both the Fabry-Perot records and the calculations, and the overall agreement is excellent. Since the Fabry-Perot technique has the best time resolution of all of the experimental techniques applied to PBX-9404 metal acceleration, the calculation of the velocity histories in Fig. 5-7 is the toughest one-dimensional test of the ignition and

growth model for detonating PBX-9404. The small differences in peak and valley velocity values may be due to several factors, including spall of the metal plates. Further experimentation and calculational model development can certainly address such physical processes on a nanosecond time scale.

The cylinder test[24] has long been used to measure the radial copper wall motion produced by detonating explosives, and calculations of this motion are then used to define the JWL equation of state parameters of the reaction products.[36] The standard streak camera technique can not record the earliest wall motion, but the Fabry-Perot technique can resolve this motion, thus enhancing the usefulness of the cylinder test. Figure 8 shows the Fabry-Perot and calculated radial copper wall velocity histories for a 0.254 cm thick copper wall driven by a 2.54 cm diameter cylindrical detonation of PBX-9404. The initial measured wall velocity is slightly less than the calculated value, which is a general trend that is not understood at the present time but the overall agreement is good. Calculations without a resolvable reaction zone are nearly identical to these ignition and growth calculations, because the effects of the thin PBX-9404 reaction zone (a reaction time of less than 20 ns or a reaction zone length of less than 0.2 mm) decay during the shock wave transit through the relatively thick copper wall. However, as will be

demonstrated for LX-17 in the next section, the inclusion of the finite thickness reaction zone is essential for cylinder test calculations for explosives with relatively thick reaction zones.

FABRY-PEROT MEASUREMENTS FOR LX-17

Four Fabry-Perot free surface velocity measurements have been made using LX-17 to accelerate thin metal plates in the 101.6 mm gas gun, and a cylinder test has also been fired. Figure 9 shows the Fabry-Perot record and the calculated free surface velocity of a 0.243 mm thick aluminum plate accelerated by 17 mm of LX-17 that was impacted by a 6 mm copper flyer plate moving at 1.89 mm/μs. This flyer velocity shocks the TATB interface to approximately 16 GPa, which results in a run distance to detonation of 5-6 mm in LX-17.[37] The calculated velocity history is initially slightly high but then closely agrees with the Fabry-Perot record for the entire 2 μs measured. The agreement is not as close in the other three experiments in which copper plates are used instead of aluminum. Figure 10 compares the measured and calculated velocities of a 0.433 mm copper plate accelerated by 14 mm of LX-17, which was initiated by 3 mm of PBX-9404 that had been impacted by a 6 mm copper flyer plate with a velocity of 1.14 mm/μs. The ignition and growth models of both PBX-9404 and

LX-17 are used in this calculation to shock initiate PBX-9404 from an initial pressure of approximately 6 GPa and then initiate the LX-17 from the PBX-9404 reactive flow. The calculated early-time velocities are slightly higher than the Fabry-Perot record, while the later-time agreement is good. This is also the case in Fig. 11 which compares measured and calculated velocity histories for 0.249 mm copper plate driven by 17 mm of LX-17 which was impacted by a 6 mm thick copper flyer plate at 1.95 mm/μs. Figure 12 shows the first 0.6 μs of the motion of a 0.1026 mm copper plate accelerated by 17 mm of LX-17 initiated by a copper flyer plate impact of 1.89 mm/μs, and again the calculated early-time motion is slightly higher than the experimentally measured motion.

This early-time disagreement could mean that the current model of the LX-17 reaction zone has the wrong pressure-time profile or is too thick. This possibility will soon be studied with multiple embedded particle velocity gauges, since the explosive mass and flyer plate mass and velocity limitations that prohibited such studies in the 101.6 mm gas gun without overdriving LX-17 with another explosive have recently been overcome. However, since the agreement with the aluminum plate velocity measurement is better than those with copper plates, the detonation wave model for LX-17 may be accurate. The high calculated early-time velocities may be due to the increased

reaction rates in the partially reacted LX-17 adjacent to the copper plate after this material is reshocked by the reflected shock wave created as the detonation wave front strikes the copper. Since the growth reaction rate has a p^3 dependence for LX-17 and the reflected pressure in the reacting LX-17 adjacent to the copper plate exceeds 60 GPa, this LX-17 reacts much more rapidly than in the steady state detonation wave, which has a reaction zone length of approximately 2 mm corresponding to a reaction time of approximately 0.25 μs. This thin layer of rapidly reacting LX-17 may then impart some additional early-time momentum to the copper plate. The reflected pressure from an aluminum plate is much lower, approximately 40 GPa, and the reaction rate in the doubly shocked LX-17 is not as rapid as in the case of copper. This effect is shown in Fig. 13, which contains calculated fraction reacted histories as various distances into LX-17 near the 0.24 mm aluminum and copper plates whose Fabry-Perot records are shown in Figs. 9 and 11, respectively. These metal plates effect the reaction rates in approximately 1 mm of LX-17 adjacent to the plates, and the stronger reflected shock wave from the copper plate increases the LX-17 reaction rate more than the reflected shock from the aluminum plate. Although the LX-17 growth reaction rate is approximately doubled by the reflected shock from the aluminum plate, the calculations predict that the reaction in the 0.125 mm of LX-17 nearest to

the aluminum is quenched before completion by the rarefaction wave created when the shock wave reaches the free surface of the aluminum. This is not predicted to occur in the copper plate calculation, since the LX-17 growth reaction rate is increased by a factor of 8 in the reflected shock wave. The problem is complicated by the fact that equations of state for the unreacted explosive and the reaction products may not be applicable at these pressures. Further experimentation with the Fabry-Perot and other techniques with very thin metal foils may eventually address these high pressure reaction rates and equation of state problems for detonating solid explosives with relatively thick reaction zones, such as LX-17. For explosives like PBX-9404 with very narrow reaction zones, experimental observation of such effects represents quite a challenge.

The Fabry-Perot technique has also been used on a LX-17 cylinder test using a 0.254 cm copper wall and a 2.54 cm diameter LX-17 charge. A prism technique[38] has also been developed to study the early wall motion. The Fabry-Perot, prism, and calculated radial copper wall velocities are compared in Fig. 14. As for PBX-9404, the initial calculated velocity is higher than the Fabry-Perot value, but then the agreement among the three curves is excellent. At later times these new experimental techniques agree with the streak camera records, and of course the reaction product JWL equation of

state is fit to that later-time expansion data. A CJ calculation without a resolved reaction zone and using a CJ pressure of 27.5 GPa for LX-17 predicts velocities much lower than the data in Fig. 14, and thus the ignition and growth ZND-type model should be used for explosives with relatively thick reaction zones. By incorporating the Fabry-Perot, prism and the ignition and growth techniques, the cylinder test has recently become an even more useful tool for measuring the metal acceleration ability of high explosives.

CALCULATIONS OF PREVIOUS PBX-9404 DATA

Since the ignition and growth model of detonating PBX-9404 accurately calculates the new multiple embedded particle velocity and stress gauge records and the Fabry-Perot metal acceleration records, it is used in this section to calculate previously reported back surface particle velocity gauge data and free surface velocity measurements on detonating PBX-9404. This particle velocity gauge data was obtained by Davis and Ramsay[32,33] using a probe consisting of 75 μm of aluminum backed by 6.35 mm of teflon that was placed behind various thicknesses of the test explosives, which are shock initiated by plane wave lenses. Figure 15 contains the five smoothed experimental particle velocity histories reported by Davis and Ramsay[32,33] for various thicknesses of PBX-9404 from 12.7 mm

to 203.2 mm and the corresponding ignition and growth calculations of the particle velocity histories in the teflon just behind the aluminum gauge. The early-time peaks in the calculated curves in Fig. 15 are caused by the detonation wave reaction zone traversing the aluminum gauge element and then entering the teflon backing. In general the calculated particle velocity histories remain higher than the experimental records for approximately 0.5 μs.

As mentioned in the Introduction, free surface velocity measurements of plates accelerated by detonating explosives have long been used to infer detonation wave parameters, such as CJ pressure and reaction zone width. The interpretation of these measurements is quite complex and has led to considerable debate.[27-31] The comparision of some of this data with ignition and growth model calculations is presented in this section. The most famous and complete free surface velocity study is the pioneering work of Craig using the reflected wire technique.[39] Craig's results are most fully discussed by Mader and Craig.[34] The measured free surface velocities of aluminum (2024 Dural) plates of various thicknesses accelerated by various thicknesses of PBX-9404 were reported as single values and then plotted as functions of plate and explosive thicknesses. The resulting curves contained changes in slope that led to various interpretations and further experimentation. Craig's measured values for Dural aluminum

plates driven by PBX-9404 detonations initiated by plane waves lenses are compared to ignition and growth calculations of these experiments in Fig. 16-19 for 1.27 cm, 2.54 cm, 5.08 cm, and 10.16 cm thick PBX-9404 charges, respectively. Various constitutive models of aluminum with different degrees of sophistication and different material property values were tested and had little effect on the peak free surface velocities, but the models did exhibit different velocity decrease or "pull-back" rates. The calculations shown in Figs. 16-19 used the 2024 Dural aluminum equation of state listed in Table II and the Steinberg-Guinan model[40] to describe the high strain rate constitutive behavior. No time dependent tensile strength or spall models were used, but such models exist and could be applied as required. The free surface velocity histories in Figs. 16-19 thus represent the maximum rate of "pull-back" that the aluminum could exhibit. It is apparent from Figs. 16-19 that Craig's measurements agree more closely with the calculated peak velocities as the length of the PBX-9404 charge increases and thus the steepness of the "pull-back," which is directly related to the steepness of the rarefaction wave in the PBX-9404 reaction products, decreases. For the steepest "pull-back" (1.27 cm PBX-9404 charges in Fig. 16), Craig's values lie 0.2-0.25 μs behind the calculated peak velocities, 0.1-0.15 μs behind for 2.54 cm charges in Fig. 17, 0.05-0.1 μs behind for 5.08 cm charges in Fig. 18, and quite

close to the peak values in Fig. 19 for 10.16 cm charges, with the exception of the 5.09 cm aluminum plate, which is most likely slowed by side rarefactions. The disagreement between the calculated and measured initial free velocities for the shortest charge lengths remains a mystery. The reflected wire technique has an inherent time response since a finite length and a finite time must be measured and differentiated to obtain a free surface velocity. The actual value of this time response is unknown. As concluded in the classical explosive metal calculational study of Lambourn and Hartley,[41] the experimental value of free surface velocity lies between the calculated initial free surface velocity and the mean velocity over the first "pull-back" period. The concept of buildup of the effective pressure from approximately 30 GPa at 1.27 cm to 37.5 GPa at 10.16 cm used by Mader[42] to calculate Craig's free surface velocity measurements does not seem to be compatible with the embedded gauge and Fabry-Perot data.

A further complication is the possibility of spall of these relatively thick aluminum plates. Veretennikov et. al.[29] demonstrated that much of the available data is consistent with approximately 1 mm of aluminum being spalled off the rest of the plate and that the dimensions of the spalled section would depend most strongly on the pressure profile in the detonating explosive and the dynamic tensile strength of the plate

material. Since the shock velocities in these aluminum plates are 7-8 mm/μs, the transit time of the shock and subsequent release wave through 1 mm of aluminum is approximately 0.25 μs. Therefore techniques, such as Fabry-Perot, that can resolve the first few nanoseconds appear to be necessary to accurately measure the initial velocity of metal acceleration by detonating explosives.

The above comparision is for aluminum plates, and further comparisons for other plate materials were made to check the conclusions reached for aluminum. Figure 20 shows Craig's measurements and the calculations for plexiglas plates driven by 10.16 cm of PBX-9404. As for aluminum, the agreement is quite close since 10.16 cm of PBX-9404 has a relatively gradual pressure decay. Two sets of free surface velocity data from the reflected wire technique are available for magnesium, although the types of magnesium used were slightly different (see Table II). Figure 21 shows Craig's measurements and the calculations for magnesium plates driven by 1.27 cm of PBX-9404, while Fig. 22 shows the Cast et. al.[35] measurements and the calculations for magnesium plates driven by 11.43 cm of PBX-9404. As shown for aluminum plates, the free surface velocity measurements from the reflected wire technique are approximately 0.25 μs down the calculated velocity history curves for 1.27 cm charges and are very close to the calculated

peak velocities for 11.43 charges. Thus the reflected wire technique results for plexiglas and magnesium are consistent with those for aluminum plates. The effects of the explosive pressure profile and the high strain rate properties of the plate material must be carefully considered when analyzing free surface velocity data for thin explosive charges.

CONCLUSIONS

Two embedded particle velocity gauge techniques, the embedded manganin stress gauge technique, and the Fabry-Perot free surface velocity measurement technique are demonstrated to yield accurate data on detonation wave propagation and metal acceleration by PBX-9404 and LX-17 in the nanosecond time resolution regime. All of these experimental results are quite consistent when compared through numerical calculations based on the ignition and growth ZND-type model of detonation. This calculational model is also compared to some previously reported back surface particle velocity gauge data and free surface velocity measurements on PBX-9404. The inclusion of the finite reaction zone length of detonation waves in ZND-type model calculations is shown to be necessary to calculate the momentum imparted to metal plates, even for PBX-9404, which has a reaction zone length of less than 0.2 mm, and especially for LX-17, which has a reaction zone length of approximately 2 mm.

The ability of PBX-9404 to attain a steady state detonation velocity and CJ pressure in less than ten millimeters of the transition to detonation is implied by the embedded gauge results, the Fabry-Perot results, and the corresponding calculations. However, the calculations do not accurately predict previously reported back surface gauge and free surface velocity data for short run distances of PBX-9404. Therefore there appears to be unresolved differences between the experimental measurements.

Both the experimental and theoretical understanding of detonation wave phenomena and the subsequent effects on inert materials are still developing. The current embedded particle velocity gauge techniques have an inherent time response of a few nanoseconds and may slightly perturb the chemical energy release rates in the explosive in contact with the gauge. These gauges and the manganin stress gauges, as well as new experimental techniques, will undoubtably yield improved data in the near future, and the numerical models can then be further refined. Continued application of Fabry-Perot and other new techniques to metal acceleration by shock initiated and detonating explosives will yield finely resolved data on equations of state and high pressure reaction rates of explosives and on high strain rate and spall phenomena of plate materials. This data can also be incorporated into

computational models. Although the complex microscopic interactions of hydrodynamics and chemical energy release that control detonation wave propagation mechanisms[43,44] are still unobservable in solid explosives, new experimental and theoretical results such as those presented in this paper are certainly producing an accurate macroscopic description of detonation wave phenomena.

TABLE I

EQUATION OF STATE AND REACTION RATE PARAMETERS FOR PBX-9404 AND LX-17

JWL EQUATION OF STATE: $p = A(1 - W/R_1V)e^{-R_1V} + B(1 - W/R_2V)e^{-R_2V} + WE/V$

	PBX-9404		LX-17	
	Unreacted Explosive	Reaction Products	Unreacted Explosive	Reaction Products
A (Mbar)	9522	8.524	778.1	6.5467
B (Mbar)	-0.05944	0.1802	-0.05031	0.071236
R_1	14.1	4.6	11.3	4.45
R_2	1.41	1.3	1.13	1.2
W	0.8867	0.38	0.8939	0.35
E (Mbar-cc/cc)		0.102		0.069
Heat Capcity (Mbar/K)	2.781×10^{-5}	1×10^{-5}	2.487×10^{-5}	1×10^{-5}
Initial Temperature (K)	298		298	
Shear Modulus (Mbar)	0.0454		0.0354	
Yield Strength (Mbar)	0.002		0.002	
Initial Density (g/cm^3)	1.842		1.895	
Detonation Wave Parameters				
Detonation Velocity (mm/μs)	8.80	8.80	7.596	7.596
Pressure (Mbar)	0.3981	0.370	0.3374	0.275
Relative Volume	0.7209	0.7406	0.6914	0.7485
Particle Velocity (mm/μs)	2.456	2.283	2.344	1.910
Reaction Rate Parameters: $\partial F/\partial t = I(1 - F)^{2/9}(\rho_s/\rho_0 - 1)^4 + G(1 - F)^{2/9}F^{2/3}p^Z$				
I (μs^{-1})	44		50	
G (μs^{-1} $Mbar^{-Z}$)	850		500	
Z	2.0		3.0	

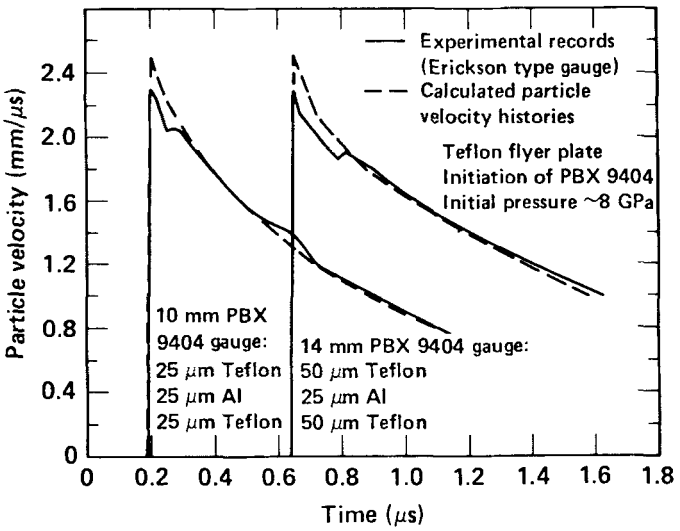

Figure 1. Embedded Erickson-type gauge and calculated particle velocity histories in detonating PBX 9404.

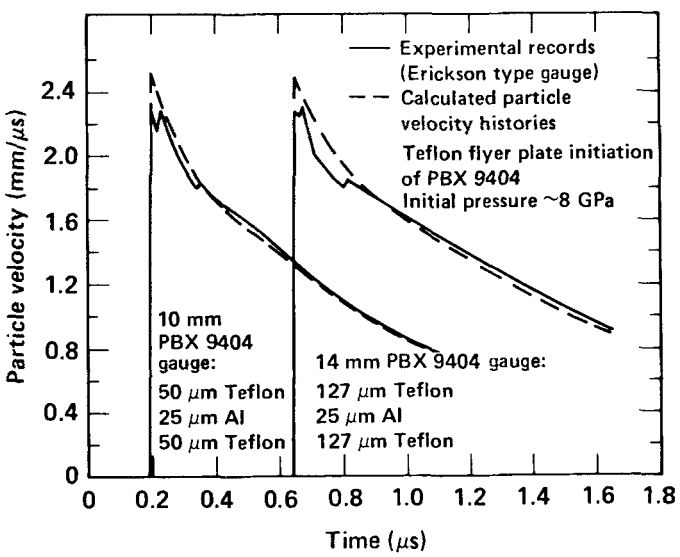

Figure 2. Additional Erickson-type embedded gauge and calculated particle velocity histories in detonating PBX 9404.

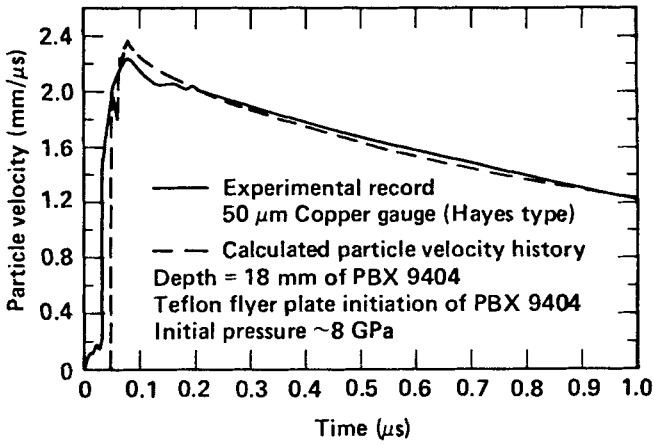

Figure 3. Hayes-type embedded gauge and calculated particle velocity histories in detonating PBX 9404.

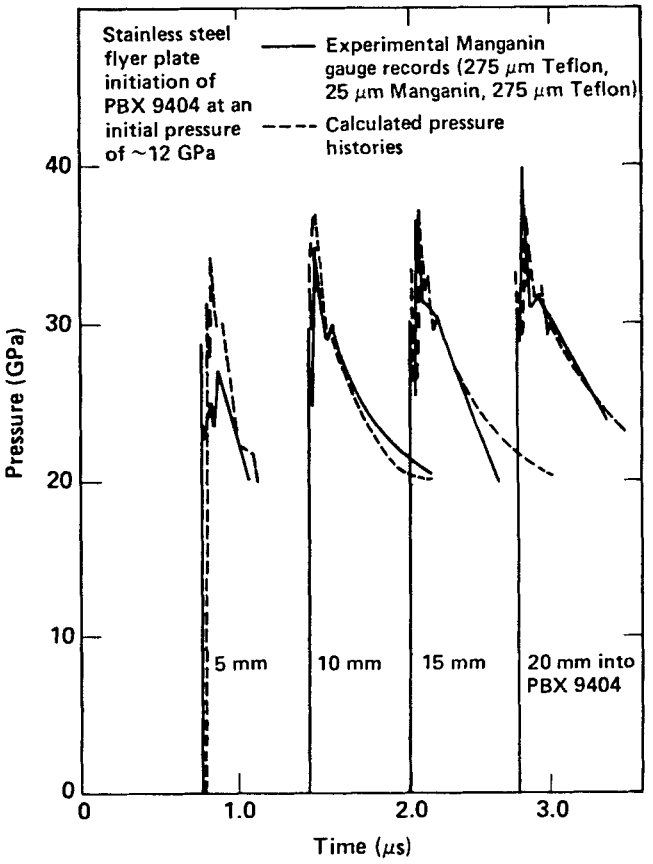

Figure 4. Embedded Manganin gauge and calculated pressure histories in detonating PBX 9404.

TABLE II
EQUATION OF STATE AND CONSTITUTIVE PROPERTIES FOR INERT MATERIALS

GRUNEISEN EQUATION OF STATE

$$P = \rho_0 c^2 \mu[1 + (1 - \gamma_0/2)\mu - (a/2)\mu^2]/[1 - (S_1 - 1)\mu - S_2\mu^2/(\mu + 1) - S_3\mu^3/(\mu + 1)^2]^2 + (\gamma_0 + a\mu)E$$

P = pressure
ρ_0 = initial density
μ = relative compression (ρ/ρ_0)
c = sound velocity
E = internal energy
γ_0, a, S_1, S_2, S_3 are constants

Material	ρ_0(g/cm^3)	c(cm/μs)	S_1	S_2	S_3	γ_0	a
Al (6061)	2.703	0.524	1.40	0	0	1.97	0.48
Al (2024 Dural)	2.785	0.5328	1.338	0	0	2.0	0.48
Copper	8.93	0.394	1.489	0	0	2.02	0.47
Teflon	2.15	0.168	1.123	3.983	-5.797	0.59	0
Magnesium (Craig)	1.775	0.4516	1.256	0	0	1.43	0.33
Magnesium (Cast)	1.738	0.452	1.233	0	0	1.54	0.33
Plexiglas (Craig)	1.186	0.2598	1.516	0	0	0.97	0

Constitutive Properties

Material	Shear Modulus (Mbar)	Yield Strength (Mbar)
Al (6061)	0.276	0.003 (0.0029 → 0.0068 in Reference 40)
Al (2024 Dural)	0.286	0.003 (0.0026 → 0.0076 in Reference 40)
Copper	0.477	0.003
Teflon	0.0279	0.002
Magnesium	0.1656	0.002
Plexiglas	0.0232	0.002

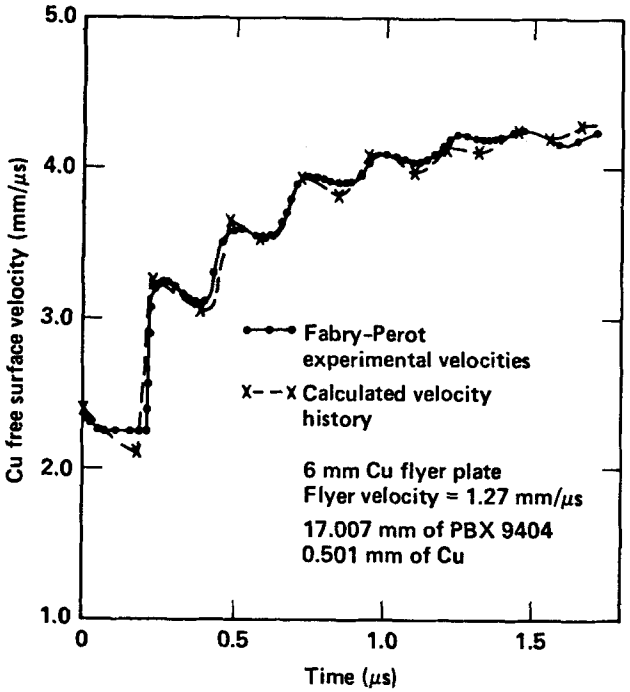

Figure 5. Fabry-Perot and calculated free surface velocity histories of a 0.501 mm copper plate accelerated by detonating PBX 9404.

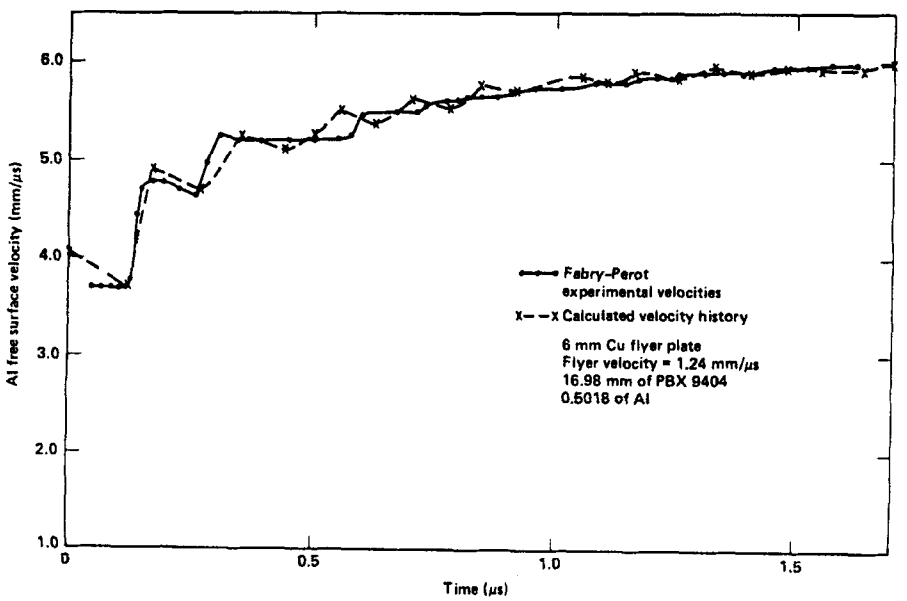

Figure 6. Fabry-Perot and calculated free surface velocity histories of a 0.5018 mm aluminum plate accelerated by detonating PBX 9404.

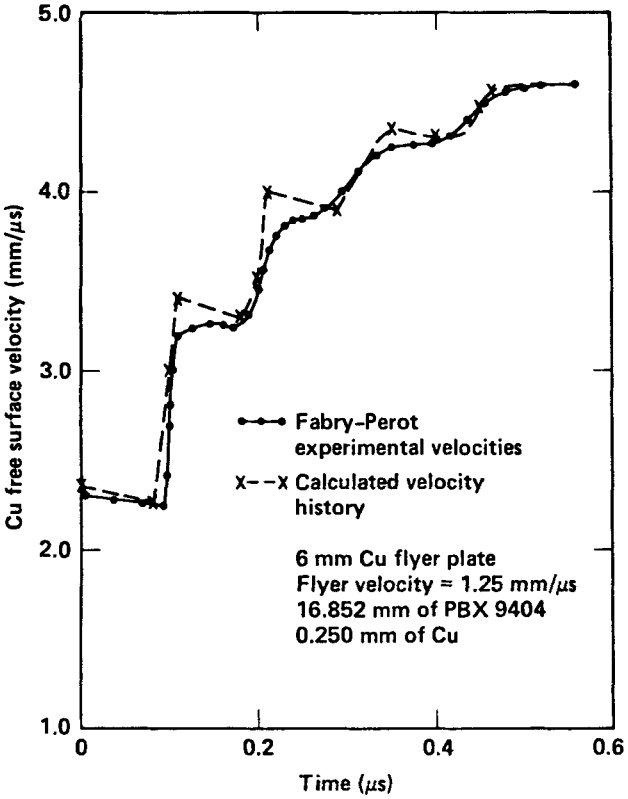

Figure 7. Fabry-Perot and calculated free surface velocity histories of a 0.250 mm copper plate accelerated by detonating PBX 9404.

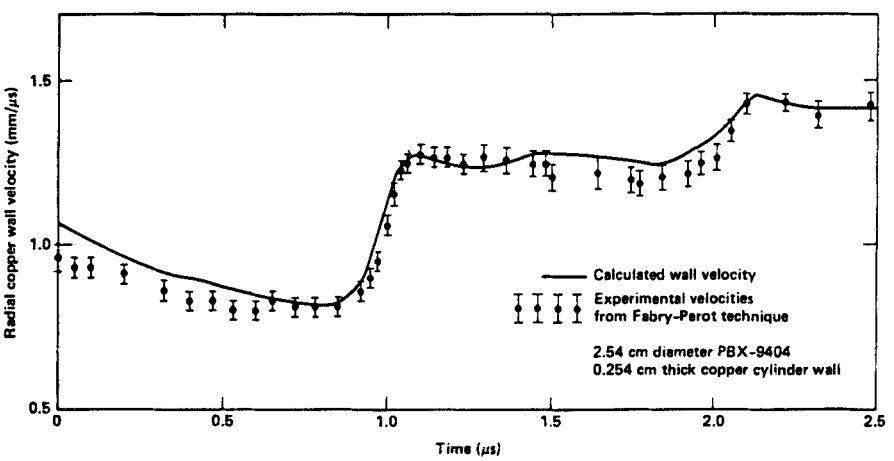

Figure 8. Fabry-Perot and calculated radial copper wall velocity histories for a PBX 9404 cylinder test.

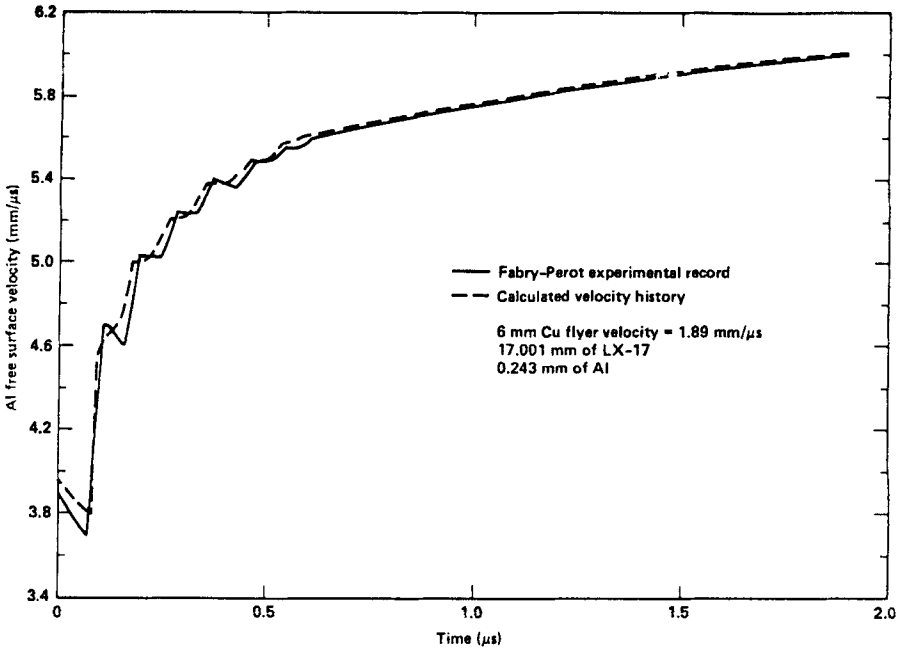

Figure 9. Fabry-Perot and calculated free surface velocity histories of a 0.243 mm aluminum plate accelerated by detonating LX-17.

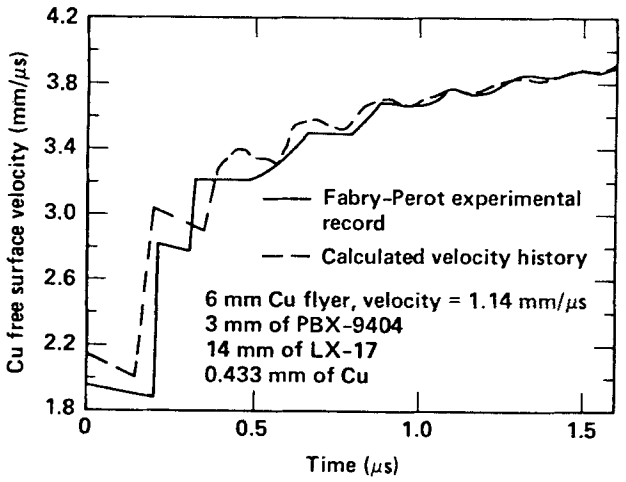

Figure 10. Fabry-Perot and calculated free surface velocity histories of a 0.433 mm copper plate accelerated by detonating LX-17 initiated by PBX 9404.

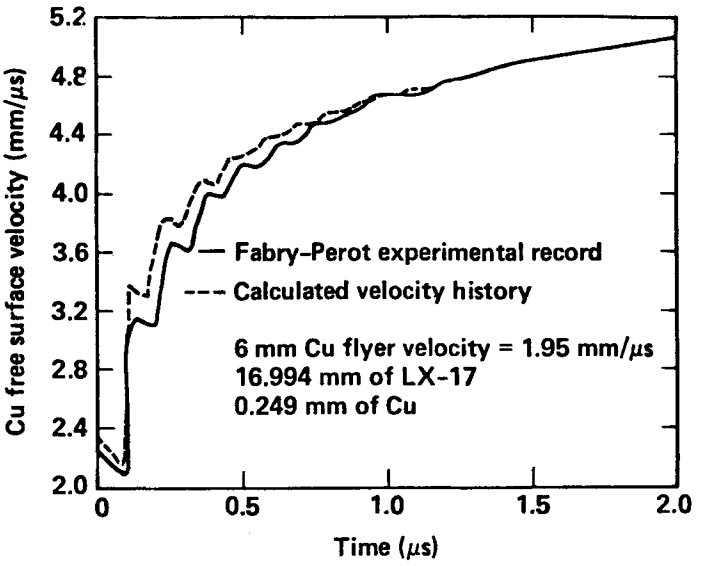

Figure 11. Fabry-Perot and calculated free surface velocity histories of a 0.249 mm copper plate accelerated by detonating LX-17.

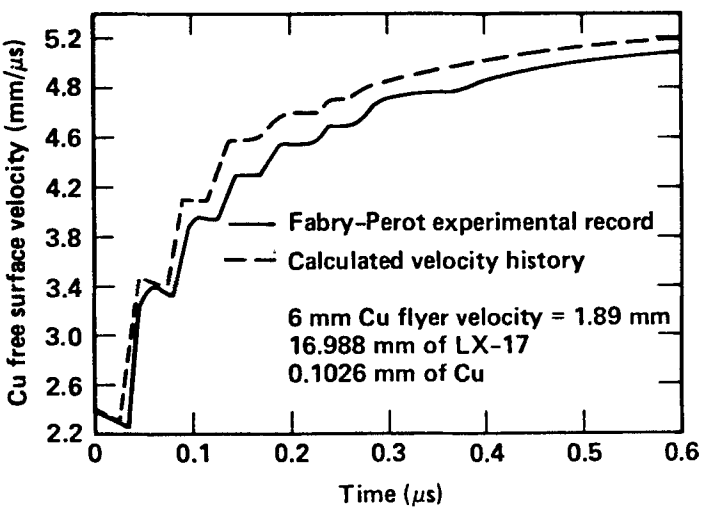

Figure 12. Fabry-Perot and calculated free surface velocity histories of a 0.1026 mm copper plate accelerated by detonating LX-17.

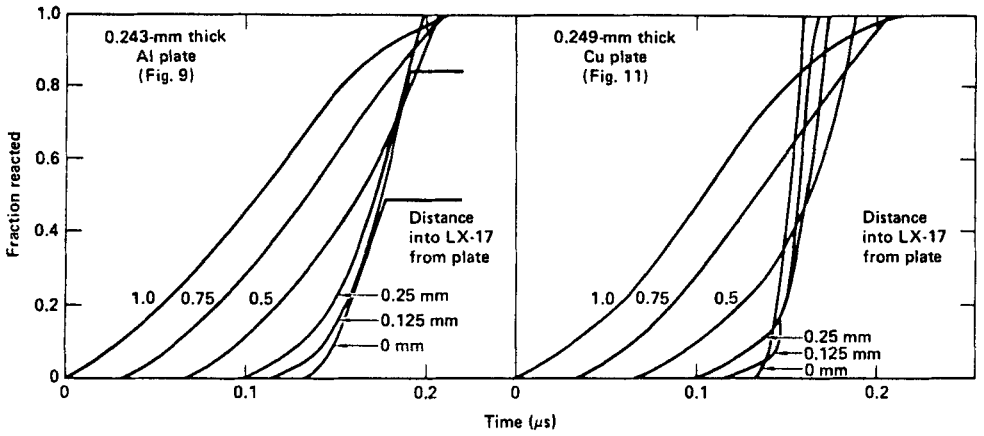

Figure 13. Calculated fraction reacted histories for LX-17 at various distances from 0.24-mm aluminum and copper plates

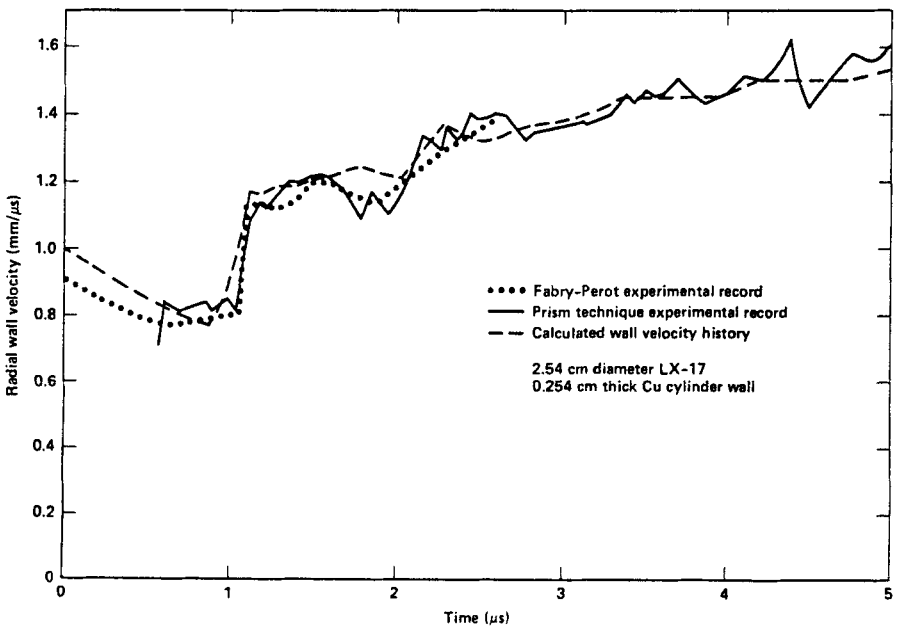

Figure 14. Fabry-Perot, prism and calculated radial copper wall velocity histories for an LX-17 cylinder test.

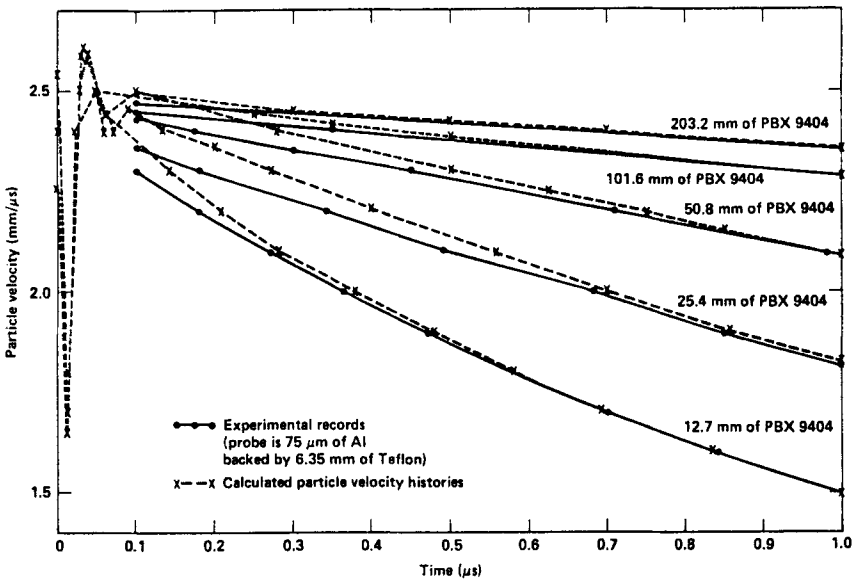

Figure 15. Particle velocity histories from detonating PBX 9404 determined by Davis' probe and the computational simulations.

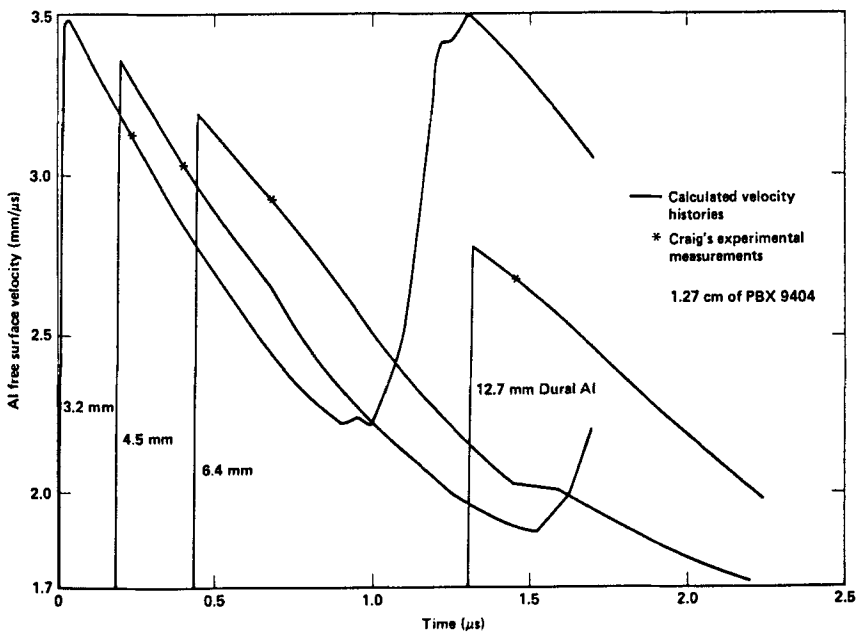

Figure 16. Craig's experimental and calculated aluminum free surface velocities for 1.27 cm PBX 9404 charges.

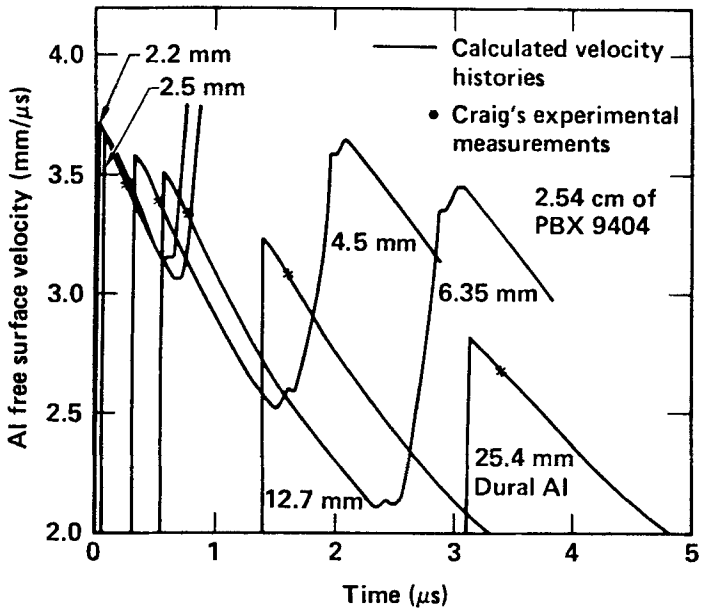

Figure 17. Craig's experimental and calculated aluminum free surface velocities for 2.54 cm PBX 9404 charges.

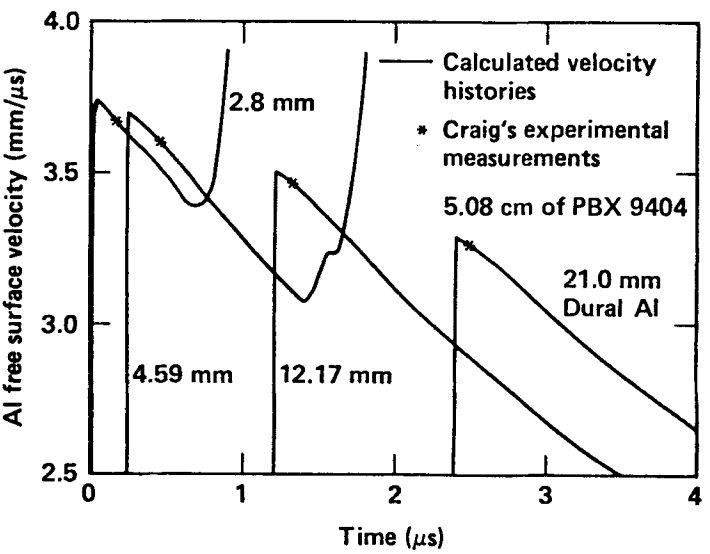

Figure 18. Craig's experimental and calculated aluminum free surface velocities for 5.08 cm PBX 9404 charges.

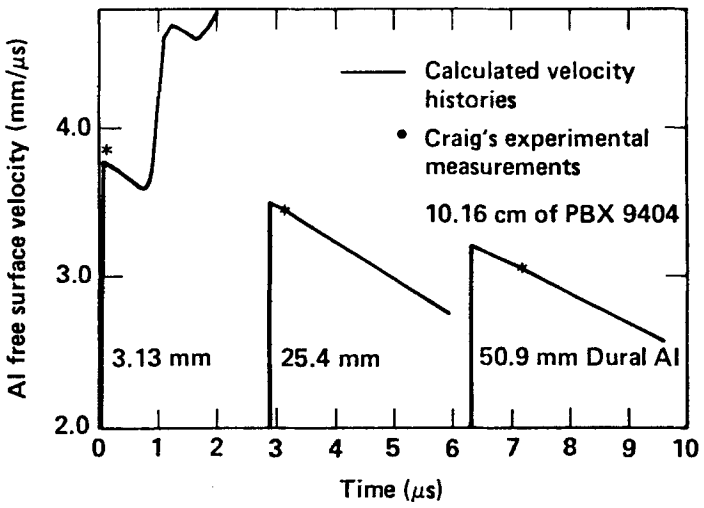

Figure 19. Craig's experimental and calculated aluminum free surface velocities for 10.16 cm PBX 9404 charges.

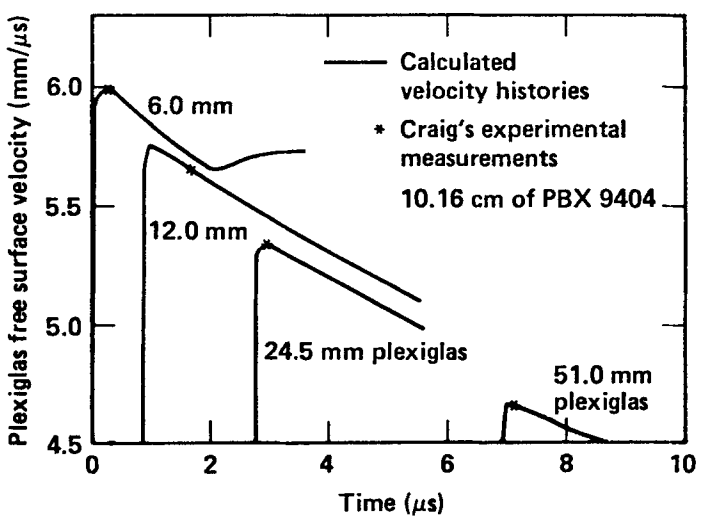

Figure 20. Craig's experimental and calculated plexiglas free surface velocities for 10.16 cm PBX 9404 charges.

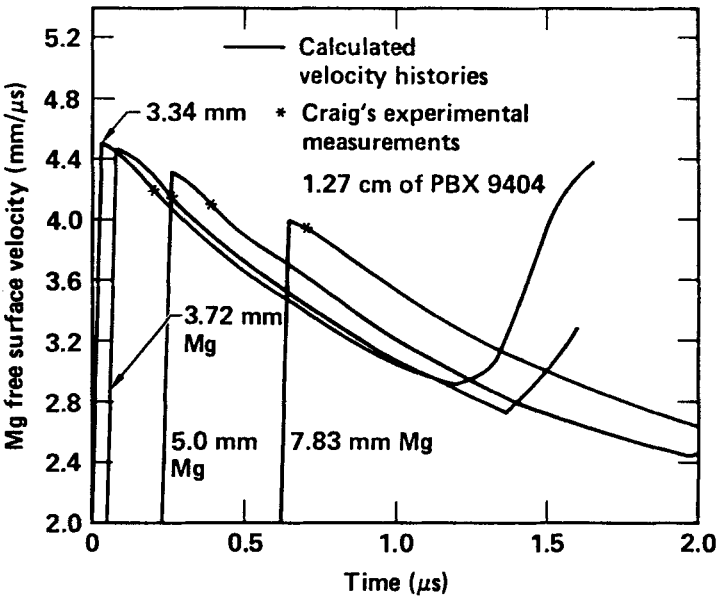

Figure 21. Craig's experimental and calculated magnesium–free surface velocities for 1.27 cm PBX 9404 charges.

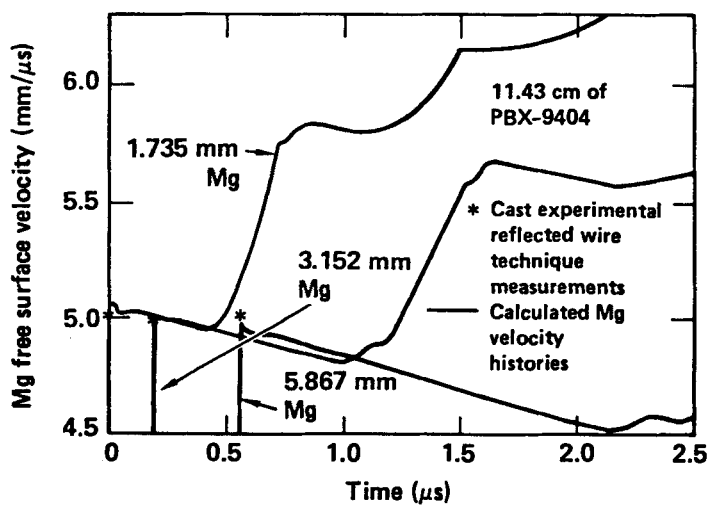

Figure 22. Cast's experimental and calculated magnesium–free surface velocities for 11.43 cm PBX 9404 charges.

This paper was prepared under the auspices of the U.S. Department of Energy at the Lawrence Livermore National Laboratory under contract No. W-7405-ENG-48.

ACKNOWLEDGMENTS

The authors would like to thank the 101.6 mm gas gun crew for its excellent experimental support, R. D. Breithaupt for the cylinder test data, and the following scientists for many stimulating discussions: S. G. Cochran, M. Finger, D. R. Goosman, L. G. Green, E. L. Lee, G. L. Nutt, W. G. Von Holle, and R. C. Weingart of LLNL; W. C. Davis and J. B. Ramsay of LANL; D. D. Bloomquist and S. A. Sheffield of SNL; and M. Cowperthwaite of SRI International.

REFERENCES

1. E. L. Lee and C. M. Tarver, Phys. Fluids 23, 2362 (1980).

2. C. M. Tarver and J. O. Hallquist, Seventh Symposium (International) on Detonation, Naval Surface Weapons Center NSWC MP 82-334, Annapolis, MD, 1981, p. 488.

3. B. Hayes and C. M. Tarver, ibid, p. 1029.

4. W. G. Von Holle and C. M. Tarver, ibid, p. 993.

5. L. G. Green, E. James, E. L. Lee, E. S. Chambers, C. M. Tarver, C. Westmoreland, A. M. Weston, and B. Brown, ibid, p. 256.

6. C. M. Tarver and P. A. Urtiew, "Theoretical Modeling of Converging and Diverging Detonation Waves in Condensed and Gaseous Explosives," paper to be presented at the Ninth International Colloquium on Dynamics of Explosions and Reactive Systems, Poitiers, France, July 1983.

7. B. M. Dobratz, "LLNL Explosives Handbook," Lawrence Livermore National Laboratory Report UCRL-52997, March 1981.

8. Y. B. Zel'dovich, J. Explt. Theor. Phys. (U.S.S.R.) 10, 524 (1940).

9. J. von Neumann, O.S.R.D. Report No. 549 (1942).

10. W. Doring, Am. Physik 43, 421 (1943).

11. D. L. Chapman, Phil. Mag. 213, Series 5, 47, 90 (1899).

12. E. Jouguet, J. Pure Appl. Math 70, Series 6, 1, 347 (1905).

13. B. Hayes, Rev. Sci. Instrum. 52 (4), 88 (1981).

14. L. M. Erickson, in "Shock Waves in Condensed Matter," (W. J. Nellis, L. Seaman and R. A. Graham, eds.) American Institute of Physics, New York, 1982, p. 685.

15. L. M. Erickson, C. B. Johnson, N. L. Parker, H. C. Vantine, R. C. Weingart, and R. S. Lee, Seventh Symposium (International) on Detonation, Naval Surface Weapons Center NSWC MP 82-334, Annapolis, MD, 1981, p. 1062.

16. M. Cowperthwaite and J. T. Rosenberg, ibid, p. 1072.

17. V. A. Veretennikov, "Measurement of the Detonation Parameters of Condensed Explosives," Chemical Physics of Processes of Combustion and Explosion: Detonation, Chernogolovka, 1980, p. 3.

18. H. Vantine, J. Chan, L. Erickson, J. Janzen, R. Weingart, and R. Lee, Rev. Sci. Instrum. 51 (1), 116 (1980).

19. A. B. Anderson, M. J. Ginsberg, W. L. Seitz, and J. Wackerle, Seventh Symposium (International) on Detonation, Naval Surface Weapons Center NSWC MP 82-334, Annapolis, MD, 1981, p. 385.

20. G. I. Kanel and A. N. Dremin, Combustion, Explosion and Shock Waves (U.S.S.R.) 13, 71 (1977).

21. R. Weingart, R. Barlett, S. Cochran, L. Erickson, J. Chan, J. Janzen, R. Lee, D. Logan, and J. T. Rosenberg, Proceedings of the Symposium on High Dynamic Pressures, Commissariat a l'Energie Atomique, Paris, 1978, p. 451.

22. J. Wackerle, R. L. Rabie, M. J. Ginsberg, and A. B. Anderson, ibid, p. 127.

23. L. M. Erickson, H. G. Palmer, N. L. Parker, and H. C. Vantine, in "Shock Waves in Condensed Matteer" (W. J. Nellis, L. Seaman, and R. A. Graham, eds.) American Institute of Physics, New York, 1982, p. 553.

24. J. W. Kury, H. C. Hornig, E. L. Lee, J. L. McDonnel, D. L. Ornellas, M. Finger, F. M. Strange, and M. L. Wilkins, Fourth Symposium (International) on Detonation, ACR-126, Office of Naval Research, White Oak, MD, 1965, p. 3.

25. S. A. Sheffield, D. D. Bloomquist and C. M. Tarver, "Subnanosecond Measurements of Detonation Fronts in Solid High Explosives," manuscript in preparation for submission for publication.

26. L. V. Al'tshuler, V. K. Ashaev, G. S. Doronin, A. D. Levin, O. N. Mironov, and A. S. Obukhov, Chemical Physics of Processes of Combustion and Explosion: Detonation, Chernogolovka, 1980, p. 8.

27. W. C. Davis, B. G. Craig and J. B. Ramsay, Phys. Fluids 8, 2169 (1965).

28. F. J. Petrone, Phys. Fluids 11, 1473 (1968).

29. V. A. Veretennikov, A. N. Dremin, O. K. Rozanov, and K. K. Shvedov, Combustion, Explosion and Shock Waves (U.S.S.R.) 3 (1), 1 (1967).

30. V. N. Zubarev, N. V. Panov, and G. S. Telegin, Combustion, Explosion and Shock Waves (U.S.S.R.) 6 (1), 102 (1970).

31. R. L. Jameson and A. Hawkins, Fifth Symposium (International) on Detonation, Office of Naval Research, ACR-184, Pasadena, CA, 1970, p.23.

32. W. C. Davis, Sixth Symposium (International) on Detonation, Office of Naval Research, ACR-221, Coronado, CA, 1976, p. 637.

33. W. C. Davis and J. B. Ramsay, Seventh Symposium (International) on Detonation, Naval Surface Weapons Center NSWC MP 82-334, Annapolis, MD, 1981, p. 531.

34. C. L. Mader and B. G. Craig, Los Alamos Scientific Laboratory, LA-5865, April 1975.

35. J. C. Cast, H. C. Hornig, and J. W. Kury, "Standard Test for Detonation Pressure Measurement," Lawrence Livermore National Laboratory Report UCRL-50645, 1970.

36. H. C. Hornig, E. L. Lee, M. Finger and J. E. Kurrle, Fifth Symposium (International) on Detonation, Office of Naval Research, ACR-184, Pasadena, CA, 1970, p. 503.

37. R. K. Jackson, L. G. Green, R. H. Barlett, W. W. Hofer, P. E. Kramer, R. S. Lee, E. J. Nidick, Jr., L. L. Shaw, and R. C. Weingart, Sixth Symposium (International) on Detonation, Office of Naval Research ACR-221, Coronado, CA, 1976, p. 755.

38. W. A. Bailey, R. A. Belcher, D. K. Chilvers, and G. Eden, Seventh Symposium (International) on Detonation, Naval Surface Weapons Center NSWC MP-82-334, Annapolis, MD, 1981, p. 678.

39. W. C. Davis and B. G. Craig, Rev. Sci. Instruments 32, 579 (1961).

40. D. J. Steinberg and M. W. Guinan, "A High-Strain-Rate Constitutive Model for Metals," Lawrence Livermore National Laboratory Report, UCRL-80465, 1978.

41. B. D. Lambourn and J. E. Hartley, Fourth Symposium (International) on Detonation, Office of Naval Research ACR-126, White Oak, MD, 1965, p. 538.

42. C. L. Mader, "Numerical Modeling of Detonations," University of California Press, Berkeley, Ca, 1979, p. 101.

43. W. Fickett and W. C. Davis, "Detonation," University of California Press, Berkeley, CA, 1979.

44. C. M. Tarver, Combustion and Flame 46, 111, 135, 157 (1982).